PHYSICAL REVIEW B **95**, 060410(R) (2017)

Completely compensated ferrimagnetism and sublattice spin crossing in the half-metallic Heusler compound $Mn_{1.5}FeV_{0.5}Al$

Rolf Stinshoff,[1] Ajaya K. Nayak,[1,2,3,*] Gerhard H. Fecher,[1] Benjamin Balke,[4] Siham Ouardi,[1] Yurii Skourski,[5] Tetsuya Nakamura,[6] and Claudia Felser[1]

[1]*Max Planck Institute for Chemical Physics of Solids, 01187 Dresden, Germany*

[2]*Max Planck Institute of Microstructure Physics, 06120 Halle, Germany*

[3]*School of Physical Science, National Institute of Science Education and Research (NISER), HBNI, Bhubaneswar, Jatni 752050, India*

[4]*Institut für Anorganische und Analytische Chemie, Johannes Gutenberg–Universität, 55099 Mainz, Germany*

[5]*Dresden High Magnetic Field Laboratory (HLD), 01328 Dresden, Germany*

[6]*Japan Synchrotron Radiation Research Institute, SPring-8, Hyogo 679-5198, Japan*

(Received 17 March 2016; revised manuscript received 14 November 2016; published 15 February 2017)

The Slater-Pauling rule states that $L2_1$ Heusler compounds with 24 valence electrons never exhibit a total spin magnetic moment. In the case of strongly localized magnetic moments at one of the atoms (here Mn) they will exhibit a fully compensated half-metallic ferrimagnetic state instead, in particular, when symmetry does not allow for antiferromagnetic order. With the aid of magnetic and anomalous Hall effect measurements, it is experimentally demonstrated that $Mn_{1.5}V_{0.5}FeAl$ follows such a scenario. The ferrimagnetic state is tuned by the composition. A small residual magnetization, which arises due to a slight mismatch of the magnetic moments in the different sublattices, results in a pronounced change of the temperature dependence of the ferrimagnet. A compensation point is confirmed by observation of magnetic reversal and sign change of the anomalous Hall effect. Theoretical models are presented that correlate the electronic structure and the compensation mechanisms of the different half-metallic ferrimagnetic states in the Mn-V-Fe-Al Heusler system.

DOI: 10.1103/PhysRevB.95.060410

Half-metallic ferromagnets are promising candidates for application in spintronics because they exhibit 100% spin polarization. They are metallic in one spin direction and semiconducting in the other [1,2]. However, ferromagnets produce a large dipole field that hinders the device performance. For example, the dipolar magnetic anisotropy becomes very large for in-plane magnetic systems leading to large switching fields. For this reason, there is a great interest in zero magnetic moment spintronics, as such systems do not produce dipole fields and are extremely stable against external magnetic fields [3–6]. The concept of half-metallic antiferromagnetism was introduced by van Leuken and de Groot [7]. It turns out, however, that symmetry does not allow half-metallic antiferromagnets and the materials are half-metallic compensated ferrimagnets [8]. Recently, Hu [9] presented a theoretical work on possible half-metallic antiferromagnets for spintronic applications. However, the identical electronic structure of both spin directions makes most of the conventional antiferromagnets unable to carry a spin-polarized current.

Heusler materials are well known for their tunable magnetic structure due to the presence of one or more magnetic sublattices. Depending on the constituting elements or crystal structure, ferromagnetic, ferrimagnetic, antiferromagnetic, or canted spin structures may be realized [10–14]. In particular, the Heusler compounds with $L2_1$ or $C1_b$ structure are well known for their half-metallic behavior [1]. These materials follow the Slater-Pauling rule [15,16] related to the half-metallicity [17–19]. According to this rule the spin magnetic moment (m) in cubic Heusler compounds with $L2_1$ structure is defined by $m = N_v - 24$, where N_v is the accumulated number of valence electrons. As a direct consequence, Heusler compounds with $N_v = 24$ never exhibit a macroscopic magnetic moment.

In certain cases, however, the DO_3 or $L2_1$ Heusler compounds with 24 valence electrons are able to exhibit a fully compensated half-metallic behavior [8]. In that concept, the Slater-Pauling rule is combined with the Kübler rule [20]. The latter states that Mn on the octahedrally coordinated position ($4b$) in Heusler compounds tends to a high, localized magnetic moment. This moment has to be completely compensated by the magnetic moments of the remaining atoms to satisfy the Slater-Pauling rule.

Although there are several theoretical predictions, most of the suggested materials either do not exist or appear only in a different crystal structure [7]. Recently it was demonstrated that a compensated ferrimagnetic state may be realized in the tetragonal Mn-Pt-Ga system [21]. However, it is known that Heusler materials with tetragonal distortion do not show half-metallicity. Kurt *et al.* [22] and Betto *et al.* [23] have shown that a compensated magnetic state with considerable spin polarization may be achieved in a cubic thin film of Mn_2Ru_xGa with composition falling between $C1_b$ and $L2_1$ Heusler compounds. Despite several attempts by different research groups, there is no experimental evidence of a compensated magnetic structure in the classical 24 valence electron based cubic Heusler compounds. In the present work it is shown by experiments and calculations that the Heusler compound $Mn_{1.5}V_{0.5}FeAl$ with $L2_1$ structure exhibits a completely compensated magnetic state. Further, the presence of a temperature and composition dependent sublattice spin compensation is demonstrated in the investigated system, while keeping the half-metallicity.

*nayak@cpfs.mpg.de

 ©2017 American Physical Society

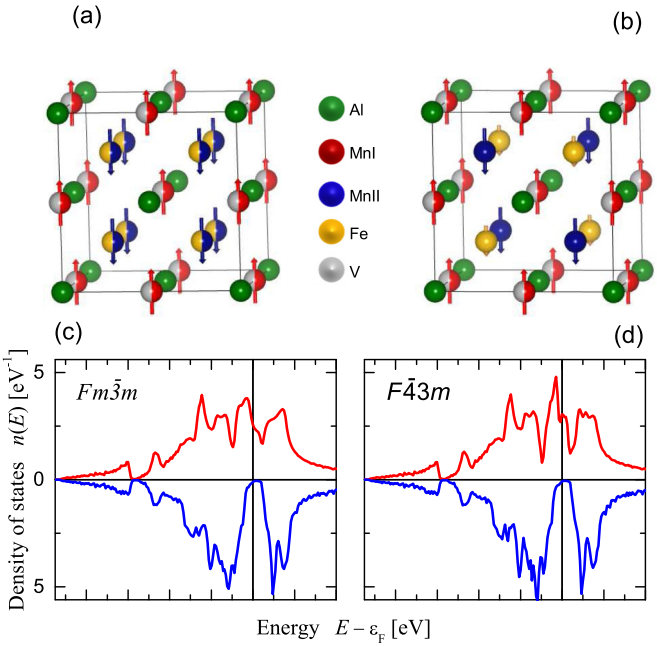

FIG. 1. Crystalline and electronic structure of $Mn_{1.5}V_{0.5}FeAl$. (a) The $L2_1$-type cubic Heusler structure with space group $Fm\bar{3}m$ (225). (b) The X-type inverse cubic Heusler structure with space group $F\bar{4}3m$ (216). Different atoms are represented by balls with different colors, shown in between the two structures. The spin resolved density of states is shown for $Fm\bar{3}m$ in (c) and for $F\bar{4}3m$ in (d).

Polycrystalline ingots of $Mn_{1.5}V_{0.5}FeAl$ were prepared by arc melting. The composition and structure of the samples was determined by energy-dispersive x-ray spectroscopy (EDX) and x-ray powder diffraction (XRD). Low field magnetic measurements were carried out by means of a vibrating sample magnetometer (MPMS 3, Quantum Design). Pulsed, high magnetic field experiments were performed at the Dresden High Magnetic Field Laboratory. The transport measurements were carried out utilizing a physical property measurement system (PPMS, Quantum Design). The electronic structure was calculated in the local spin density approximation. The self-consistent electronic structure calculations were carried out using the spin-polarized fully relativistic Korringa-Kohn-Rostocker (SPRKKR) method provided by Ebert *et al.* [24,25].

The XRD and EDX analysis indicates that $Mn_{1.5}V_{0.5}FeAl$ crystallizes in a single phase cubic Heusler structure with a lattice parameter of $a = 5.83$ Å. A detailed structural analysis has been presented in the Supplemental Material [26]. The two most energetically favored crystal structures are shown in Figs. 1(a) and 1(b) together with their magnetic order. In the regular $L2_1$ cubic Heusler structure with space group $Fm\bar{3}m$ (225), the Al atoms occupy the 4*a* position, the 4*b* position is equally occupied by V and Mn atoms, and a statistical distribution of the Mn and Fe atoms at 8*c* is expected. In a less probable situation, an ordering of the Mn and Fe atoms can split the 8*c* position to 4*c* and 4*d*, as shown in Fig. 1(b). In order to determine the density of states (DOS) of $Mn_{1.5}V_{0.5}FeAl$, the calculations were performed using SPRKKR with coherent potential approximation (CPA) to account for the random occupation of the sites and for chemical disorder. Comparing the total energies at the same lattice parameter, one finds that the energy of the $L2_1$ structure with space group $Fm\bar{3}m$ [Fig. 1(a)] is 0.5 meV lower compared to the X structure with space group $F\bar{4}3m$ [Fig. 1(b)]. The electronic structure reveals clearly the half-metallic character of $Mn_{1.5}V_{0.5}FeAl$ for both structure types with chemical disorder. The gap in the minority DOS is defined by the states of the Mn atoms located on the 8*c* and the Fe atoms located on the 8*c* or 4*c* positions. This coincides with previous calculations for various Heusler compounds, as in most cases, the gap is dominated by the states arising from the atom on the 8*c* site [19]. The calculated magnetic moments of $Mn_{1.5}FeV_{0.5}Al$ are listed in Table I. A summation of the site specific magnetic moments yields a zero total moment, as expected for a completely compensated ferrimagnet. For more details regarding the calculations, see the Supplemental Material [26].

TABLE I. Site specific magnetic moments in $Mn_{1.5}FeV_{0.5}Al$. The calculations were carried out by means of SPRKKR-CPA using the $L2_1$ structure ($Fm\bar{3}m$, 225) or the X-type structure ($F\bar{4}3m$, 216). All magnetic moments are given in μ_B. The total moments are given per primitive cell. The site specific spin m_s and orbital m_l magnetic moments are given per atom. Note the rounding; the induced moment at Al is $<0.006\mu_B$.

	225			216		
Atom	Site	m_s	m_l	Site	m_s	m_l
Mn	(8*c*)	1.40	0.03	(4*d*)	1.38	0.03
Fe	(8*c*)	0.28	0.02	(4*c*)	0.35	0.03
Mn	(4*b*)	−2.79	−0.01	(4*b*)	−2.86	−0.01
V	(4*b*)	−0.55	0.01	(4*b*)	−0.60	0.01
Al	(4*a*)	−0.01	−0.00	(4*a*)	−0.01	−0.00
$m_{tot}^{s,l}$		0.003	0.046		0.000	0.058
m_{tot}		0.05			0.06	

Figure 2(a) shows the temperature dependence of the magnetization $M(T)$ for a completely compensated sample. As expected, the magnetization vanishes at 0 K as is typical for a completely compensated ferrimagnet. The magnetization stays close to zero up to about 50 K. The Curie temperature appears at about 335 K.

$M(T)$ curves measured for a slightly overcompensated sample in different induction fields are shown in Fig. 2(b). From the $M(T)$ curves measured in an induction field of 0.1 T a Curie temperature (T_C) of about 308 K is determined. By decreasing the temperature the magnetization first completely reduces to zero at 127 K and then increases again by lowering the temperature below 127 K. This type of magnetic behavior indicates the presence of a compensation point of the ferrimagnetic order. The completely compensated behavior is very sensitive to the composition of the sample as will be shown next.

The temperature dependencies of the total and the sublattice magnetic moments were simulated using a molecular field model for a two-sublattice ferrimagnet. In particular, the equations introduced by Stearns [27] for binary compounds (Fe_3Al, Fe_3Si) with Heusler-type structure were used. This model may come close to the $L2_1$ structure with space group

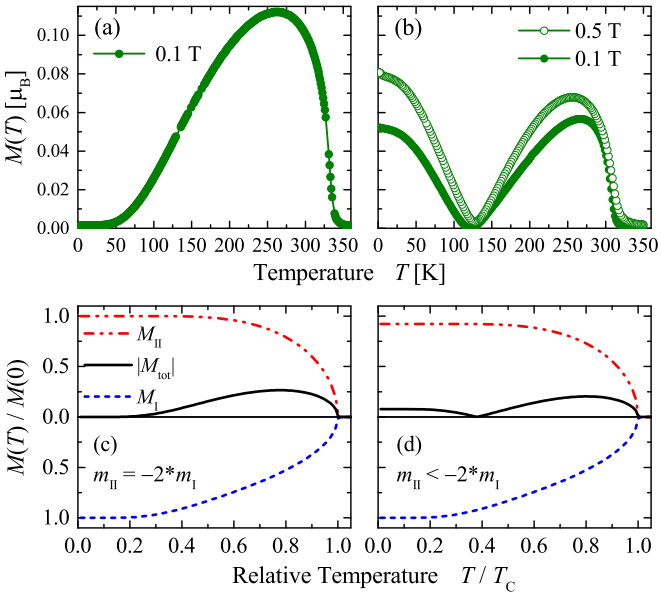

FIG. 2. Magnetization of $Mn_{1.5}FeV_{0.5}Al$. (a) shows the temperature dependence of the magnetization $M(T)$, measured for a completely compensated sample. (b) shows the temperature dependence of the magnetization measured for an overcompensated sample in different fields. The theoretical behavior of a two-sublattice ferrimagnet in the molecular field approximation is shown in (c) and (d): (c) shows the magnetization for a completely compensated ferrimagnet with $|m_{II}| = |2m_I|$; (d) shows the case with $|m_{II}| < |2m_I|$. m_i are the average magnetic moments of the atoms on the ith sublattice at $T = 0$.

225. It is assumed that the magnetic moment m_I of the atoms in sublattice I is smaller (half) but that twice as many atoms are occupying lattice I. That is, lattice I describes the 8c site, whereas lattice II corresponds to the 4b sites with higher magnetic moments m_{II} but only half as many atoms ($n_I/n_{II} = 2$) compared to lattice I. The completely compensated ferrimagnet appears when $n_I m_I = n_{II} m_{II}$. The exchange integrals J_{ij} should be largest for interactions between the atoms in sites I and II. Further, the exchange integrals between atoms of type I should be much smaller compared to the atoms of type II, with the latter being close to those between type I and II atoms. In particular, it was assumed that $J_I/J_{I-II} = 1/2$ and $J_{II}/J_{I-II} = 2/3$. The results are shown in Figs. 2(c) and 2(d) that compare the completely compensated case with a slightly overcompensated case. Figure 2(c) describes a ferrimagnet where the compensation point appears at $T = 0$ and the magnetization stays nearly zero up to about $T/T_C \approx 1/5$. For $m_{II} < |2m_I|$, a compensation point appears [Fig. 2(d)]. The latter is classified as a Néel N-type ferrimagnet [28].

Figure 3 shows the field dependence of the magnetization for two different temperatures, at the maximum of the magnetization (263 K) and close to zero (2 K). At high temperatures the material appears very soft but has a small remanence and coercive field at low temperature. Inset (b) shows that the coercive field is constant below 50 K where the magnetization vanishes [compare Fig. 2(a)]. Above this critical temperature, the magnetization softens with increasing temperature. The

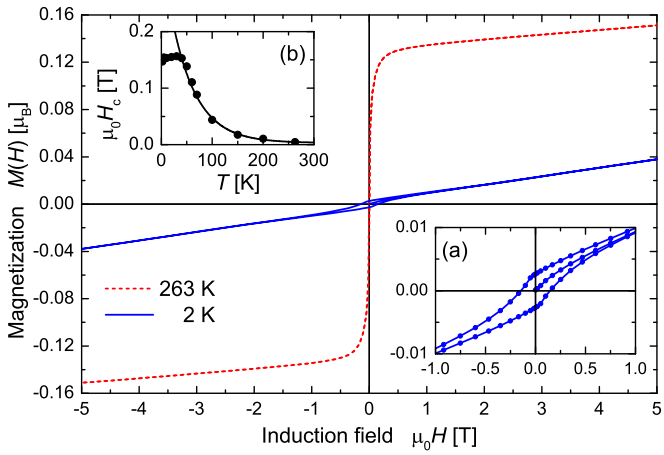

FIG. 3. Field dependent magnetization of $Mn_{1.5}FeV_{0.5}Al$. Shown is the magnetization $M(H)$ at 2 and 263 K. Inset (a) shows the low temperature behavior on an enlarged scale. Inset (b) shows the temperature variation of the coercive field.

appearance of a coercive field is a typical effect at the compensation point [29]. In certain cases it is assumed to diverge at the compensation point, whereas it clearly saturates below the critical temperature in the completely compensated half-metallic ferrimagnet.

So far the occurrence and some magnetic properties of a completely compensated half-metallic ferrimagnet is demonstrated. The compensation phenomenon is better studied, however, in the slightly overcompensated sample with a compensation point at a finite temperature. The remaining part is thus devoted to this case.

The $M(H)$ loops measured at different temperatures demonstrate the compensation phenomenon [Fig. 4(a)] in the overcompensated sample. A nearly linear hysteresis loop with almost zero spontaneous magnetization is found in the vicinity

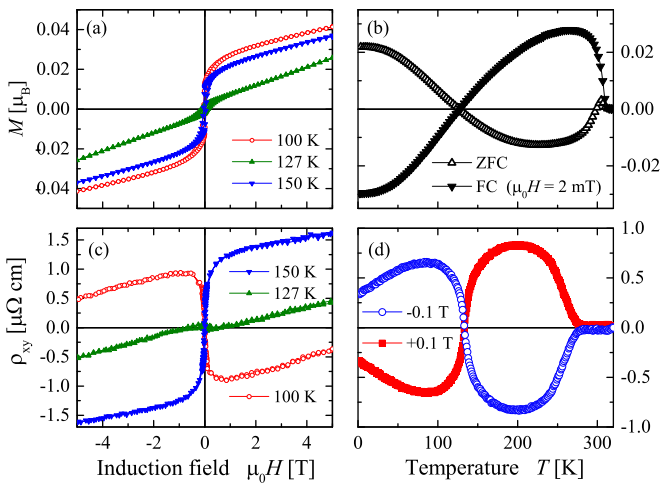

FIG. 4. Magnetic and transport properties of overcompensated $Mn_{1.5}FeV_{0.5}Al$. (a) Isothermal magnetization loops, $M(H)$, at different temperatures. (b) ZFC and FC $M(T)$ curves measured in a small field of 2 mT. (c) Field dependence of the Hall effect measured at different temperatures. (d) Temperature dependence of Hall resistivity measured at ±0.1 T.

of the compensation temperature (127 K). The $M(H)$ loops measured for temperatures below and above the compensation point exhibit a soft magnetic behavior. The most important point is that both $M(T)$ and $M(H)$ measurements hint at a saturation magnetization that is less than $0.1\mu_B$ away from the compensation point. This suggests that the sample virtually exhibits a nearly compensated magnetic state over the full temperature range.

It is seen from Fig. 2(b) that the minimum at the compensation point shifts slightly with increasing induction field. For a deeper understanding of this effect we have measured zero-field-cooled (ZFC) and field cooled (FC) $M(T)$ curves in a very small field of 2 mT [Fig. 4(b)]. In this case the FC curve, which shows a positive magnetization at higher temperature, crosses the temperature axis at 127 K to give a negative magnetization at low temperatures. The ZFC curve follows an exactly opposite behavior to that of the FC curve. The zero crossing of the magnetization clearly indicates a sublattice magnetic compensation at 127 K. Similar magnetic reversal at the compensation point has been observed in systems with spin-orbital compensation [30]. Pulsed magnetic field measurements at 1.5 K and at the compensation point (127 K) show a linear magnetic response with fields up to 55 T without any spin-flop transition (see Supplemental Material [26]). This clearly indicates a strong exchange coupling between the different magnetic sublattices in $Mn_{1.5}V_{0.5}FeAl$.

The magnetic measurements shown in Figs. 2(a) and 2(b) only give an indication of a sublattice spin crossing at the compensation point. Anomalous Hall effect (AHE) measurements have been performed at different temperatures, to allow for a direct observation of the spin crossing across the compensation point (see Fig. 4). The AHE measured at 50 and 100 K shows a negative sign, i.e., negative (positive) value in positive (negative) field. At the compensation point the AHE becomes virtually zero. Above the compensation point for $T = 150$ and 200 K, a positive anomalous Hall effect is observed. The change in sign of the AHE can be seen in the temperature dependence of the AHE measured in a field of ± 0.1 T [Fig. 4(d)]. The AHE changes from a negative (positive) maximum around 100 K to a positive (negative) maximum at 200 K when measured in a field of 0.1 T (-0.1 T). The two curves cross the zero line at about 130 K. Since the AHE is an intrinsic property of ferro- and ferrimagnets, a small uncompensated moment below and above the compensation point will result in a nonvanishing AHE. The most important point is that the AHE changes its sign, which clearly indicates the change of the sublattice magnetic structure across the compensation point. The AHE is an intrinsic manifestation of a Berry curvature, that changes due to the change of the sublattice magnetic moment from spin up to spin down, resulting in a change of the sign across the compensation point. A further analysis of the anomalous Hall effect across the compensation point is given in the Supplemental Material [26].

In conclusion, the existence of a completely compensated ferrimagnetic state in the half-metallic $L2_1$ cubic Heusler compound $Mn_{1.5}V_{0.5}FeAl$ has been experimentally demonstrated. Although there have been several theoretical works regarding realization of a fully compensated magnetic state in the $L2_1$ cubic Heusler compounds with 24 valence electrons, no successful experimental attempt has been made until now. This work also establishes the existence of a temperature dependent sublattice spin crossing in half-metallic ferrimagnets. The compensation temperature can be varied by an intentional variation of the stoichiometry. Recently, it has been demonstrated that antiferromagnets may be utilized as a principal component in spintronic devices, especially in tunnel magnetoresistance based devices. The present half-metallic compensated ferrimagnet adds the advantage of nearly 100% spin polarization, which is extremely important for spintronics.

The authors thank N. Demitri for assistance during the XRD experiment at ELETTRA. This work is funded by the Deutsche Forschungsgemeinschaft (project 1.3-A in research unit 1464 *ASPIMATT*) and by the ERC Advanced Grant (Grant No. 291472) *Idea Heusler*. The experiments at the High Magnetic Field Laboratory Dresden (HLD) were supported by Euro-MagNET II under the European Union Contract No. 228043. X-ray diffraction measurements were performed at beamline XRD1 of the ELETTRA Synchrotron (Trieste, Italy) under Proposal No. 20145509.

[1] R. A. de Groot, F. M. Mueller, P. G. van Engen, and K. H. J. Buschow, Phys. Rev. Lett. **50**, 2024 (1983).

[2] M. I. Katsnelson, V. Yu. Irkhin, L. Chioncel, A. I. Lichtenstein, and R. A. de Groot, Rev. Mod. Phys. **80**, 315 (2008).

[3] Y. Soh, and R. K. Kummamuru, Philos. Trans. R. Soc., A **369**, 3646 (2011).

[4] B. G. Park, J. Wunderlich, X. Marti, V. Holy, Y. Kurosaki, M. Yamada, H. Yamamoto, A. Nishide, J. Hayakawa, H. Takahashi, A. B. Shick *et al.*, Nat. Mater. **10**, 347 (2011).

[5] Y. Y. Wang, C. Song, B. Cui, G. Y. Wang, F. Zeng, and F. Pan, Phys. Rev. Lett. **109**, 137201 (2012).

[6] X. Marti, I. Fina, C. Frontera, J. Liu, P. Wadley, Q. He, R. J. Paull, J. D. Clarkson, J. Kudrnovsky, I. Turek *et al.*, Nat. Mater. **13**, 367 (2014).

[7] H. van Leuken and R. A. de Groot, Phys. Rev. Lett. **74**, 1171 (1995).

[8] S. Wurmehl, H. C. Kandpal, G. H. Fecher, and C. Felser, J. Phys.: Condens. Matter **18**, 6171 (2006).

[9] X. Hu, Adv. Mater. **24**, 294 (2012).

[10] P. J. Webster and K. R. A. Ziebeck, in *Alloys and Compounds of d-Elements with Main Group Elements. Part 2*, edited by H. P. J. Wijn, Landolt-Börnstein—Group III Condensed Matter Vol. 19C (Springer-Verlag, Heidelberg, 1988), pp. 104–185.

[11] K. R. A. Ziebeck and K.-U. Neumann, in *Alloys and Compounds of d-Elements with Main Group Elements. Part 2*, edited by H. P. J. Wijn, Landolt-Börnstein—Group III Condensed Matter Vol. 32C (Springer-Verlag, Heidelberg, 2001), pp. 64–314.

[12] J. Kübler, *Theory of Itinerant Electron Magnetism* (Clarendon, Oxford, 2000).

[13] T. Graf, C. Felser, and S. S. P. Parkin, Prog. Solid State Chem. **39**, 1 (2011).
[14] C. Felser and A. Hirohata, in *Heusler Alloys*, Springer Series in Materials Science Vol. 222 (Springer International Publishing, Cham, 2016).
[15] J. C. Slater, Phys. Rev. **49**, 931 (1936).
[16] L. Pauling, Phys. Rev. **54**, 899 (1938).
[17] I. Galanakis, P. H. Dederichs, and N. Papanikolaou, Phys. Rev. B **66**, 174429 (2002).
[18] G. H. Fecher, H. C. Kandpal, S. Wurmehl, C. Felser, and G. Schönhense, J. Appl. Phys. **99**, 08J106 (2006).
[19] H. C. Kandpal, G. H. Fecher, and C. Felser, J. Phys. D: Appl. Phys. **40**, 1507 (2007).
[20] J. Kübler, A. R. Williams, and C. B. Sommers, Phys. Rev. B **28**, 1745 (1983).
[21] A. K. Nayak, M. Nicklas, S. Chadov, P. Khuntia, C. Shekhar, A. Kalache, M. Baenitz, Y. Skourski, V. K. Guduru, A. Puri *et al.*, Nat. Mater. **14**, 679 (2015).
[22] H. Kurt, K. Rode, P. Stamenov, M. Venkatesan, Y.-C. Lau, E. Fonda, and J. M. D. Coey, Phys. Rev. Lett. **112**, 027201 (2014).
[23] D. Betto, N. Thiyagarajah, Y.-C. Lau, C. Piamonteze, M.-A. Arrio, P. Stamenov, J. M. D. Coey, and K. Rode, Phys. Rev. B **91**, 094410 (2015).
[24] H. Ebert, in *Fully Relativistic Band Structure Calculations for Magnetic Solids Formalism and Application*, edited by H. Dreysee, Electronic Structure and Physical Properties of Solids. The Use of the LMTO Method, Lecture Notes in Physics Vol. 535 (Springer-Verlag, Berlin, Heidelberg, 1999), pp. 191–246.
[25] H. Ebert, D. Ködderitzsch, and J. Minar, Rep. Prog. Phys. **74**, 096501 (2011).
[26] See Supplemental Material at http://link.aps.org/supplemental/10.1103/PhysRevB.95.060410 for details on structural study, additional magnetization and transport measurements and electronic structure calculations.
[27] M. B. Stearns, Phys. Rev. **168**, 588 (1968).
[28] L. Néel, Science **174**, 985 (1971).
[29] D. J. Webb, A. F. Marshall, Z. Sun, T. H. Geballe, and R. M. White, IEEE Trans. Magn. **24**, 588 (1988).
[30] J. W. Taylor, J. A. Duffy, A. M. Bebb, M. R. Lees, L. Bouchenoire, S. D. Brown, and M. J. Cooper, Phys. Rev. B **66**, 161319(R) (2002).